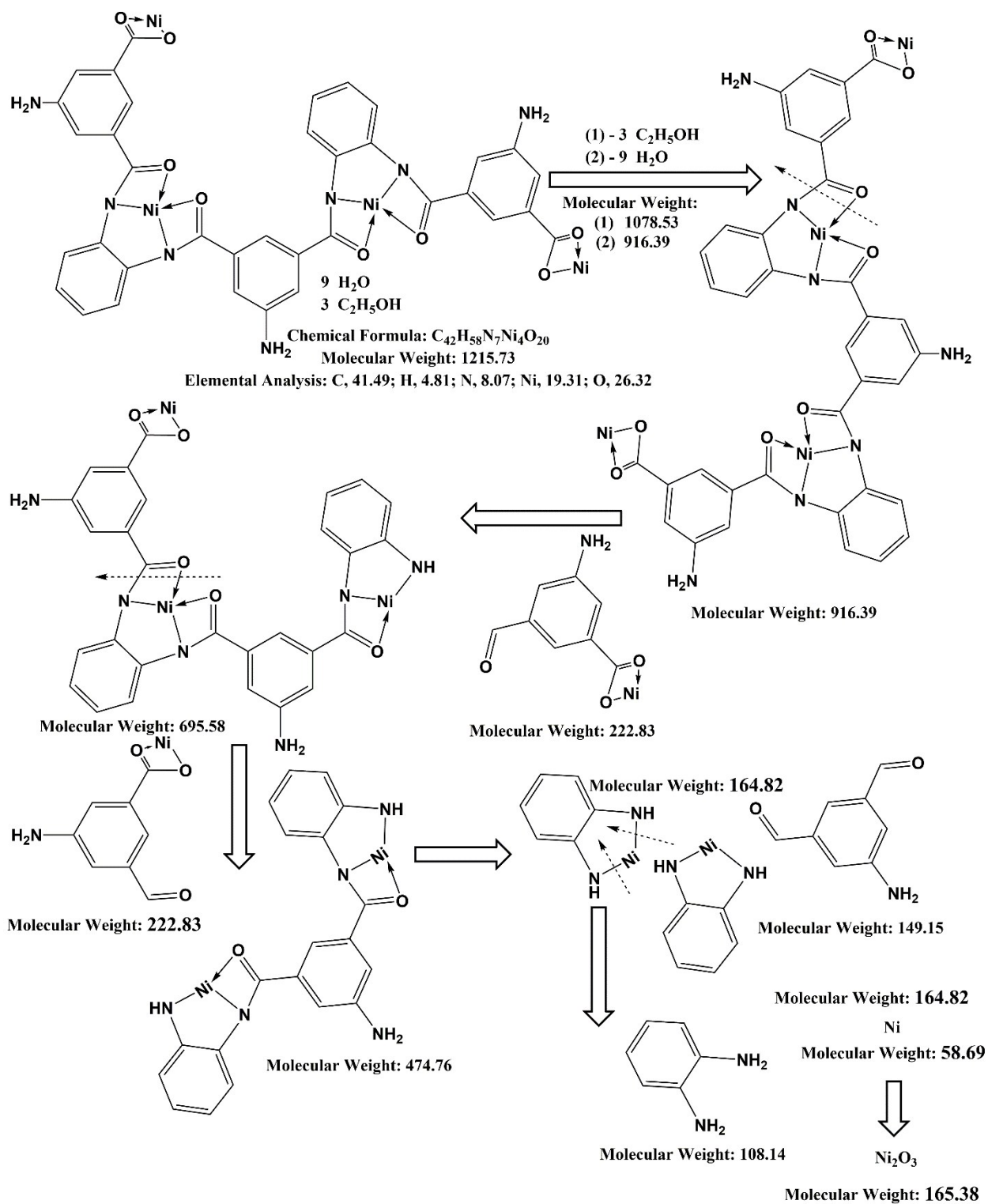


Scheme S1: The proposed mechanism of the nano linker (NL) and Ni-MOF synthesis.



Scheme S2: The proposed fragmentation scheme of the nickel metal-organic framework (Ni-MOF).

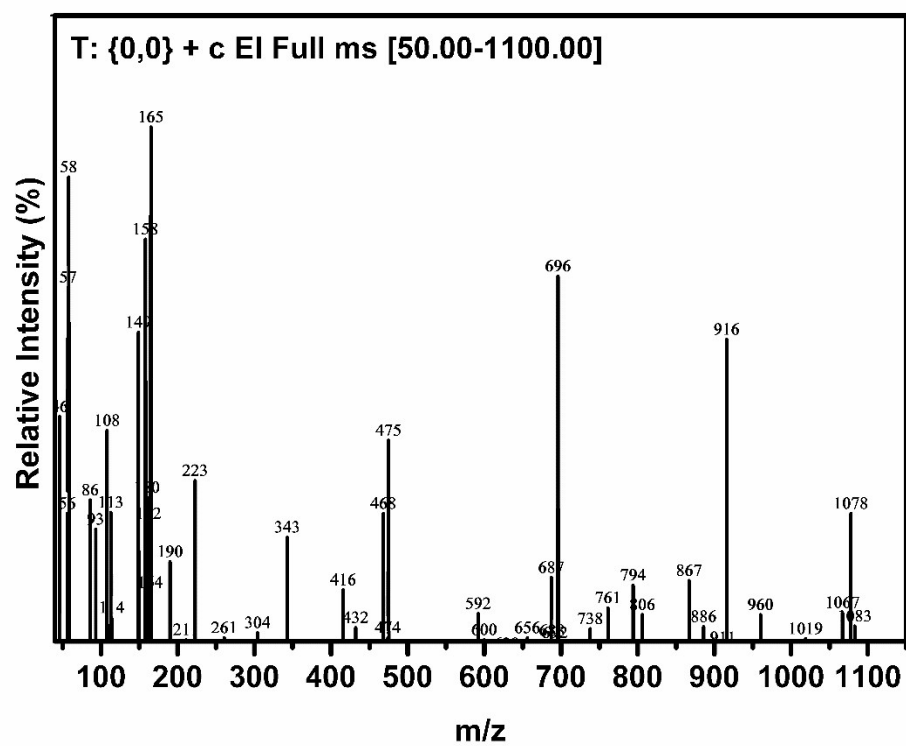


Fig. S1: The mass spectrum of the nickel metal-organic framework (Ni-MOF).

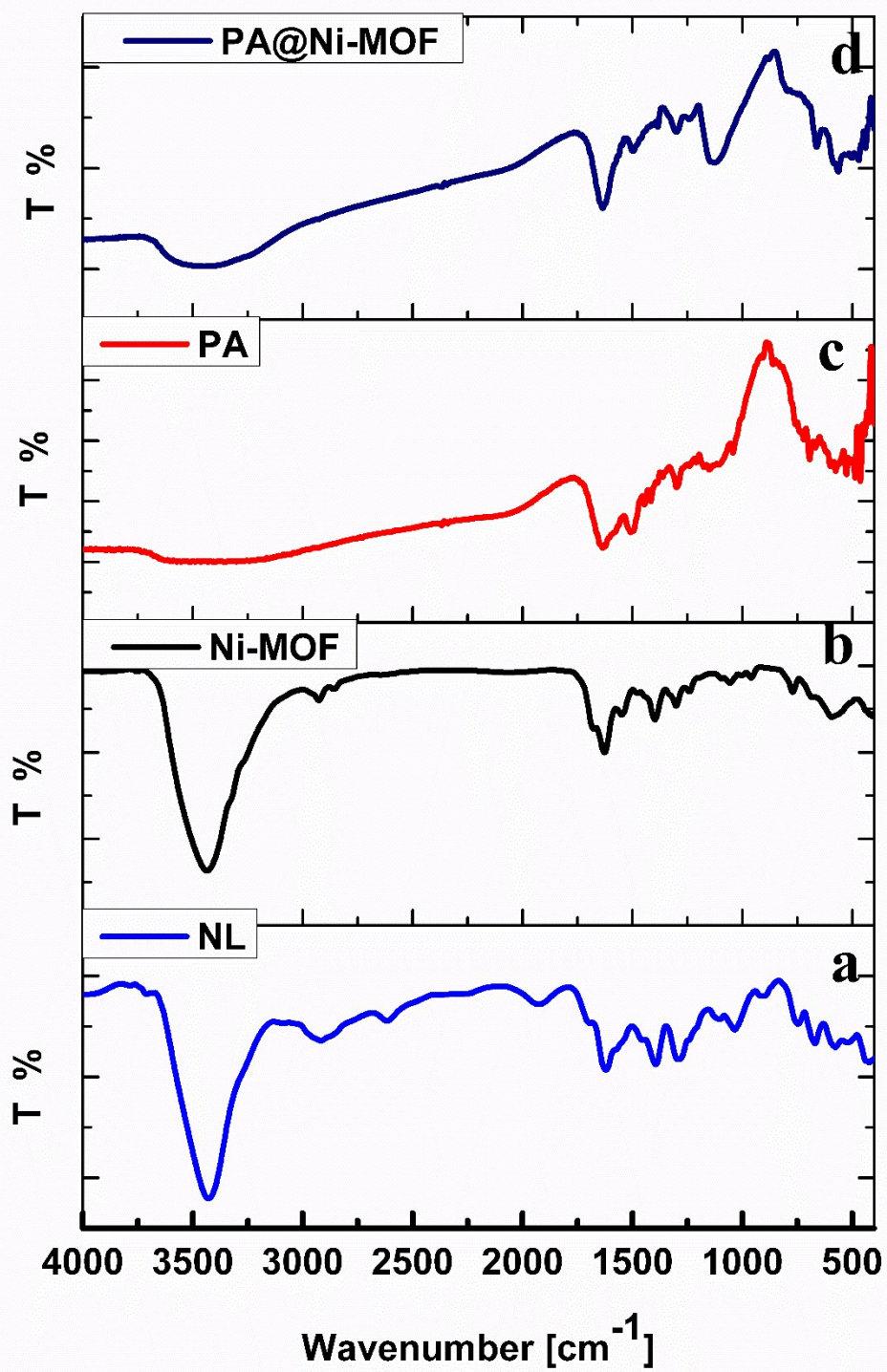


Fig. S2: The FT-IR spectra of NL, Ni-MOF, PA and PA@MOF composite.

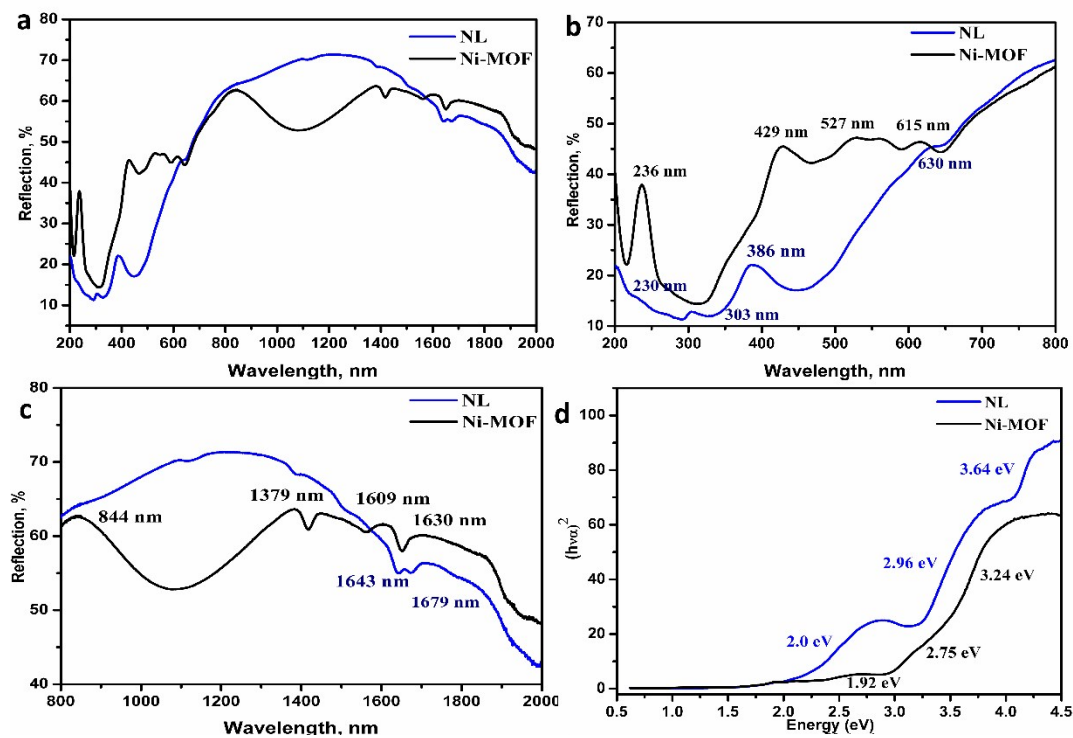


Fig. S3: (a, b, and c) The electronic absorption spectra of NL and Ni-MOF at different ranges, (d) The band gap energy of NL and Ni-MOF.

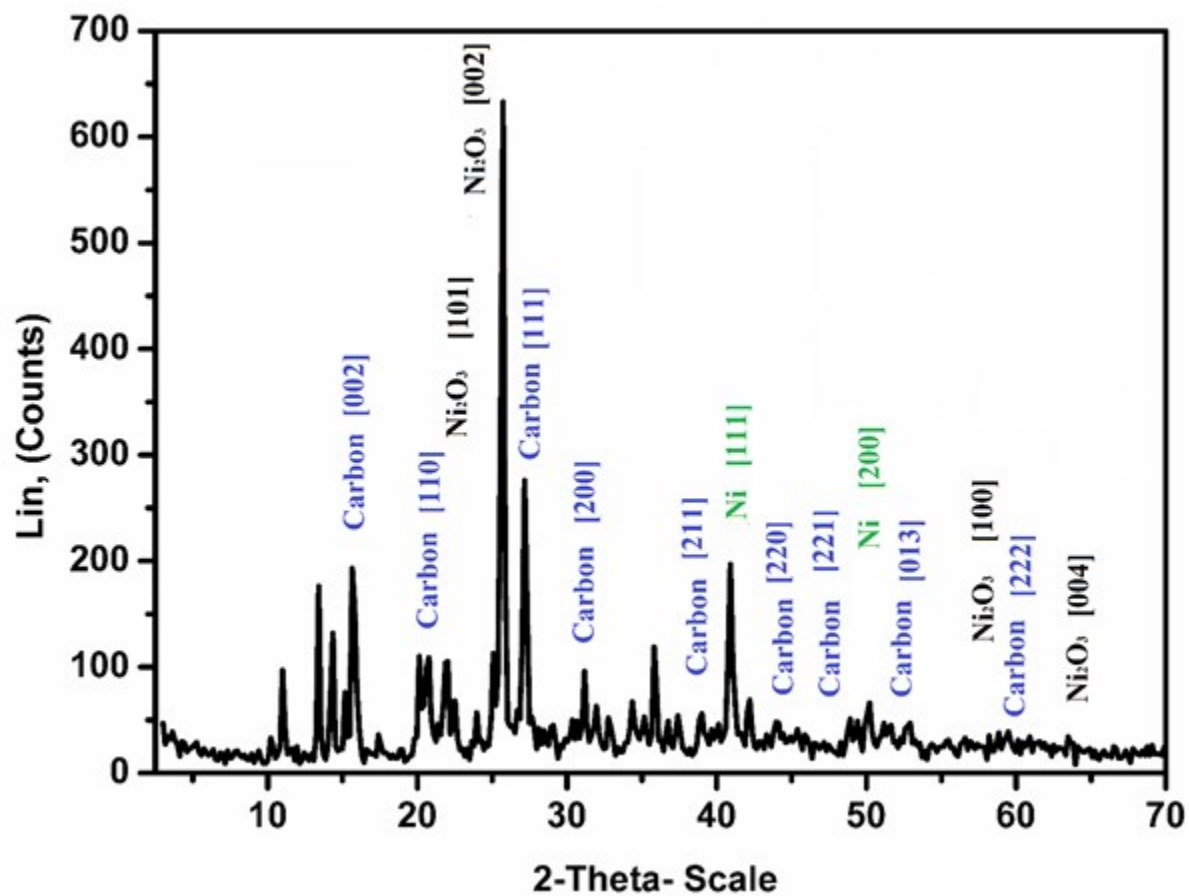


Fig. S4: The X-ray diffraction spectra of Ni-MOF.

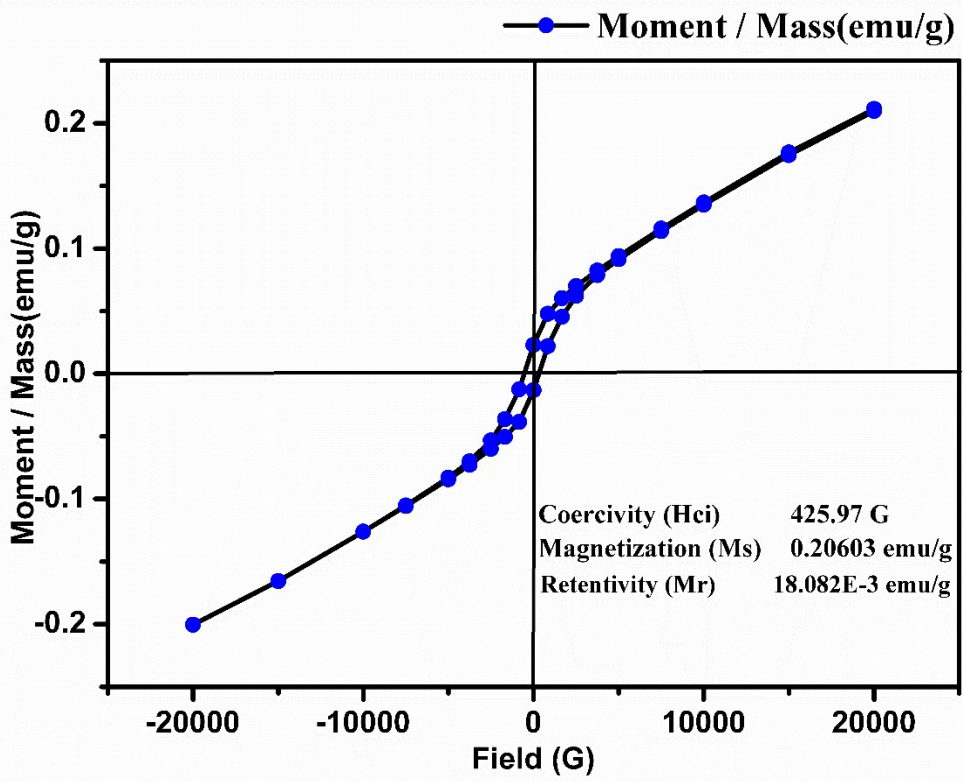


Fig. S5: The magnetization curve of the Ni-MOF.

Table S1: Summary of XRD data, Miller indices and interplanar distances of Ni-MOF

Peak No.	2 θ	Intensity Count	Intensity %	d value A $^\circ$	θ (Radians)	Sin θ	Sin $^2 \theta$	Ratio 1	Ratio 2	(hkl)
1	10.369	13	2.68	8.524491	0.090487	0.09036	0.008166	1	2	
2	11.176	24.3	5.01	7.910699	0.097529	0.09737	0.009482	1.1612	2.3224	
3	13.581	163	33.6	6.514753	0.118517	0.11824	0.013981	1.4745	2.9489	
4	14.381	51.5	10.6	6.154093	0.125498	0.12517	0.015667	1.1206	2.2412	
5	15.788	58	12	5.608675	0.137776	0.13734	0.018863	1.2039	2.4078	
6	17.56	14.5	2.99	5.046486	0.15324	0.15264	0.023299	1.2352	2.4704	
7	20.408	62.4	12.9	4.348208	0.178093	0.17715	0.031383	1.347	2.6939	
8	20.894	35.5	7.32	4.248152	0.182335	0.18133	0.032879	1.0477	2.0953	
9	21.944	63	13	4.047197	0.191498	0.19033	0.036225	1.1018	2.2035	
10	22.465	14.4	2.97	3.9545	0.196044	0.19479	0.037943	1.0474	2.0948	
11	24.053	18.4	3.79	3.696895	0.209902	0.20836	0.043416	1.1442	2.2884	
12	25.216	33.2	6.85	3.528962	0.220051	0.21828	0.047646	1.0974	2.1948	
13	25.808	485	100	3.449339	0.225217	0.22332	0.049871	1.0467	2.0934	104
14	27.39	373	76.9	3.253597	0.239023	0.23675	0.056052	1.1239	2.2478	110
15	28.996	18.3	3.77	3.076939	0.253038	0.25035	0.062673	1.1181	2.2362	
16	31.17	40	8.25	2.867111	0.27201	0.26867	0.072182	1.1517	2.3034	
17	33.112	17.3	3.57	2.703259	0.288957	0.28495	0.081198	1.1249	2.2497	113
18	34.459	23.1	4.76	2.600609	0.300712	0.2962	0.087734	1.0805	2.1610	
19	35.941	24.8	5.11	2.4967	0.313644	0.30853	0.095189	1.085	2.1699	202
20	40.888	43.1	8.89	2.20532	0.356815	0.34929	0.122005	1.2817	2.5634	24
21	42.88	12	2.47	2.10737	0.374199	0.36553	0.13361	1.0951	2.1902	116
22	44.067	23.3	4.8	2.053319	0.384557	0.37515	0.140737	1.0533	2.1066	122
23	50.288	37.6	7.75	1.81292	0.438846	0.42489	0.180536	1.2828	2.5655	214
24	51.454	16.2	3.34	1.774543	0.449021	0.43408	0.188429	1.0437	2.0874	300
25	69.797	4.24	0.87	1.346386	0.609094	0.57212	0.327326	1.7371	3.4742	

Table S2: EDX analysis of the Ni-MOF.

Element	Weight %	Atomic %	Net Int.	Error %
C	41.8	51.35	104.99	8.16
N	8.32	7.97	5.06	27.78
O	30.97	36.09	94.41	11.38
Ni	18.91	4.59	28.95	13.44

Table S3: Recovery of the electrochemical HCV RNA biosensor for the determination of the target RNA in spiked human serum samples.

Samples	Added	Found*	Recovery (%)	RSD (%)
Sample-1	1 fM	0.967 fM	96.7	4.6
Sample-2	10 pM	0.942 pM	94.2	3.7
Sample-3	100 nM	99.63 nM	99.63	2.9

*The values found are the average of three measurements; RSD, the relative standard deviation.

2.1. Materials

1, 2-phenylenediamine $C_6H_8N_2$; 99.5%; and $NiCl_2 \cdot 6H_2O$; 99.99%, DMF, glacial acetic acid, ethanol Aniline, hydrochloric acid (HCl), ammonium persulphate $(NH_4)_2S_2O_8$, acetone, sodium chloride (NaCl), potassium chloride (KCl), ferric chloride ($FeCl_3$), sodium phosphate dibasic (Na_2HPO_4), potassium dihydrogen phosphate (KH_2PO_4) and RNA oligonucleotides were purchased from Sigma Aldrich. 5-aminoisophthalic acid $C_8H_7NO_4$; 98%; bovine serum albumin (BSA), potassium ferricyanide ($K_3Fe(CN)_6$) and potassium ferrocyanide ($K_4Fe(CN)_6$) were supplied from Across organics and Merck. The DNA oligonucleotides sequences are HCV probe: 5'-TACCACAAGGCCTTTCGCGACCCAACA-3' HCV target: 5'-TGTTGGGTCGCGAAAGGCCTTGTGGTA-3' Non-complementary nucleic acid: 5'-CGATGGTTGACAGACGGTGACCG-3'. All the nucleic acids were dissolved in phosphate buffer solution (PBS) (pH 7.4). The other reagents are of analytical grade and were used without further purification.

2.2. Instruments

The characterization and applications were performed using different analytical techniques: The FE-SEM images and EDX spectroscopy spectra were recorded with a combination of a field emission scanning electron microscope (FE-SEM), and element mapping by a spatially resolved energy-dispersive X-ray spectrometer (EDX) (JEOL JSM-6510LV, Japan). The mass spectra of solid Ni-MOF were recorded using a Thermo Scientific- ISQ single quadrupole mass spectrometer (Thermo Scientific, USA). The Fourier-transform infrared (FT-IR) spectra were recorded with a JASCO FT/IR-460 spectrophotometer with the use of KBr tablets in the range from 400 to 4000 cm^{-1} at room temperature (JASCO, USA). Elemental analysis (C-H-N) was performed using a Costech ECS-4010- analyzer (Costech, Italy). The UV-vis spectra were obtained using V-770 UV-Visible/NIR spectrophotometer over a range from 200 to 2200 nm (JASCO, USA), and the band gap was calculated with Optbandgap-204B soft wear. The X-ray diffraction (XRD) analysis of Ni-MOF was performed with a D8-AVANCE X-ray diffractometer (Bruker, Germany) with Cu-K α radiation ($\lambda = 0.154056$ nm) for identification of the crystalline phase, relative crystallinity, and crystal size of as-prepared Ni-MOF, The XRD analysis was performed in the 2θ range from 3.105° to 70.086° with a 0.020° step at a scan speed of 0.4 s. The crystallite size was calculated from XRD data by means of the Scherrer equation. The oxidation states and species in the prepared

materials were recorded by a Thermo Scientific™ K-Alpha™ X-ray photoelectron spectrometer (XPS) (Thermo Scientific, USA), using Al-K α micro-focused monochromator within an energy range up to 4 KeV. Thermal analysis, Differential Scanning Calorimetry/Thermogravimetric Analysis (DSC/TGA) of the samples was carried out with a Universal V4.5-TA Instruments (USA), with a rate of 10 °C min⁻¹. The magnetic properties of the fabricated samples were measured using a vibrating sample magnetometer (7400-1 VSM, USA) in a maximum applied field of 20 kOe. All the electrochemical measurements, including cyclic voltammetry (CV) and electrochemical impedance spectroscopy (EIS), were performed on a potentiostat (Autolab PGSTAT) and the data were analyzed with Origin-8. A conventional three-electrode system was used in this work. Glassy carbon electrode was employed as a working electrode (GCE, 3 mm in diameter), silver/silver chloride (Ag/AgCl) was the reference electrode and platinum was the counter electrode.